

# HENRY

Hydraulic Engineering Repository

Ein Service der Bundesanstalt für Wasserbau

---

Conference Paper, Published Version

## **Slunyaev, Alexey; Sergeeva, Anna; Pelinovsky, Efim; Talipova, Tatiana Numerical Simulation of Rogue Waves in Coastal Waters**

Zur Verfügung gestellt in Kooperation mit/Provided in Cooperation with:  
**Kuratorium für Forschung im Küsteningenieurwesen (KFKI)**

---

Verfügbar unter/Available at: <https://hdl.handle.net/20.500.11970/108465>

Vorgeschlagene Zitierweise/Suggested citation:

Slunyaev, Alexey; Sergeeva, Anna; Pelinovsky, Efim; Talipova, Tatiana (2016): Numerical Simulation of Rogue Waves in Coastal Waters. In: Yu, Pao-Shan; Lo, Wie-Cheng (Hg.): ICHE 2016. Proceedings of the 12th International Conference on Hydroscience & Engineering, November 6-10, 2016, Tainan, Taiwan. Tainan: NCKU.

### **Standardnutzungsbedingungen/Terms of Use:**

Die Dokumente in HENRY stehen unter der Creative Commons Lizenz CC BY 4.0, sofern keine abweichenden Nutzungsbedingungen getroffen wurden. Damit ist sowohl die kommerzielle Nutzung als auch das Teilen, die Weiterbearbeitung und Speicherung erlaubt. Das Verwenden und das Bearbeiten stehen unter der Bedingung der Namensnennung. Im Einzelfall kann eine restriktivere Lizenz gelten; dann gelten abweichend von den obigen Nutzungsbedingungen die in der dort genannten Lizenz gewährten Nutzungsrechte.

Documents in HENRY are made available under the Creative Commons License CC BY 4.0, if no other license is applicable. Under CC BY 4.0 commercial use and sharing, remixing, transforming, and building upon the material of the work is permitted. In some cases a different, more restrictive license may apply; if applicable the terms of the restrictive license will be binding.

Verwertungsrechte: Alle Rechte vorbehalten

## Numerical Simulation of Rogue Waves in Coastal Waters

*Alexey Slunyaev<sup>1</sup>, Anna Sergeeva<sup>1</sup>, Efim Pelinovsky<sup>1</sup>, Tatiana Talipova<sup>1</sup>, Dong-Jiing Doong<sup>2</sup>*

1. Department of Nonlinear Geophysical Processes, Institute of Applied Physics, and Nizhny Novgorod State Technical University, Nizhny Novgorod, Russia

2. Department of Hydraulic and Ocean Engineering, National Cheng Kung University, Tainan, Taiwan

### ABSTRACT

In this paper we review the ongoing research on developing procedures which allow realistic reconstructions of sea states and extreme waves, including so-called rogue waves recorded in Taiwanese coastal waters. We confine the approach to the assumption of unidirectional wave propagation; the focus is made on the spatio-temporal evolution of surface waves. Some examination of limits of applicability of the reconstruction method, and elements of the short-term forecasting are presented. The potential usefulness of the stochastic simulations of irregular wind waves is discussed.

**KEY WORDS:** numerical simulations; wave dynamics reconstruction; short-term forecasting; extreme events; rogue waves; nonlinear wave kinematics; finite water depth.

### INTRODUCTION

The rogue (or freak) waves are a threat that has been recognized rather recently, and nowadays attracts much attention, see for reviews (Kharif and Pelinovsky, 2003; Dysthe et al., 2008; Kharif et al., 2009; Slunyaev et al., 2011). The number of in-situ registrations of rogue wave is still insufficient, and many related questions (dominating mechanisms, probability of accuracy, favourable sea conditions, possibility of prediction, etc) still challenge trustworthy answers.

Measurements of the surface elevation at a certain point provide only limited information about waves. In this paper we discuss an approach to reconstruct the lacking wave data with the purpose to complete the picture of extreme wave dynamics. Numerical reconstructions of the wave dynamics on the basis of instrumental records were performed in (Trulsen, 2001; Divinsky et al., 2004; Slunyaev et al., 2005, 2014; Slunyaev, 2006; Sergeeva et al, 2014). As a result, not only the full detailed wave information in the vicinity of the measurement point can be obtained, but the rogue wave evolution can be also recovered.

In this paper we show at first how the reconstruction technique may be applied, using a record from the Taiwanese coastal water. The direct verification of the reconstruction procedure requires in-situ measurements at several downstream locations, which are not available at present. Instead, in the second section we use strongly nonlinear simulations as the reference, and validate our approximate approach. In the last section we discuss possible applications of the realistic

simulations of stochastic sea waves, and present some results of analysis of the spatio-temporal wave data of strongly nonlinear wave simulations over different depths, which at present can be hardly obtained from laboratory measurements.

### RECONSTRUCTION OF IN-SITU ROGUE WAVE REGISTRATIONS

In this section we use the general idea that a time series of the surface elevation recorded in one point may be used to reconstruct the wave dynamics in the vicinity of the registration point, if only one major assumption is applied, that the waves in the position of registration are unidirectional. If so, then the surface displacement and potential on the surface are related, and the momentary velocity may be calculated (in our work we generally use the nonlinear theory for modulated waves, the extended nonlinear Schrodinger (NLS) framework, see Slunyaev et al (2014)). When the full information on waves is available in one point (i.e., the surface displacement  $\eta(x_0, t)$  and the surface velocity potential  $\varphi^s(x_0, t)$ ), then the equations which integrate the evolution in space are most convenient (the boundary problem). Different equations may be applied for the simulation in space: linear equations, equations for weakly nonlinear weakly modulated waves (modifications of the NLS theory), spatial modifications of the Zakharov equations.

The nonlinear Schrodinger equation (NLSE) is the simplest nonlinear theory for modulated waves. The coefficients of the equation depend on the local depth, and thus vary in case when waves propagate over slowly changing bathymetry. For this problem the NLSE may be written in form

$$i \frac{dB}{dx} = -i\mu \frac{d(kh)}{dx} B - \frac{i}{c_g} \frac{dB}{dt} + \lambda \frac{d^2 B}{dt^2} + \nu |B|^2 B, \quad (1)$$

where  $B(x, t)$  is the complex amplitude of the envelope. The surface displacement and surface velocity potential are in the leading order

$$\eta = \text{Re}(B \exp(i\omega t - ikx)), \quad \varphi^s = \frac{g}{\omega} \text{Im}(B \exp(i\omega t - ikx)). \quad (2)$$

Here  $x$  is the horizontal coordinate directed onshore ( $x = 0$  corresponds to the shoreline and the wave gauge is situated at  $x = x_0$ ),  $t$  denotes the time;  $\omega$  and  $k$  are the carrier frequency and wavenumber;  $g$  is the

gravity acceleration. When the water depth  $h$  is constant, equation (1) reduces to the classic NLSE with shoaling coefficient  $\mu = 0$ . The term with  $\mu$  is responsible for the conservation of wave energy flux  $c_g|B|^2$ , where  $c_g$  is the group velocity.

Eq. 1 may be used for reconstruction of waves which propagate strictly onshore with wave crests aligned with depth isolines. While waves propagate over variable depth, the carrier frequency remains constant,  $\omega = \omega_0$ , and the wavenumber  $k$  varies in accordance with the dispersion relation  $\omega^2 = gk \tanh(kh)$ , hence it is a function of  $x$ ,  $k = k(h(x))$ .

In Sergeeva et al (2014) we applied this framework for reconstruction of a few registrations of abnormally high waves, which were selected from the bank of long-term instrumental measurements near the coasts of Taiwan (Doong et al., 2007). The conditions of wave registration correspond to the sloping bottom, see Fig. 1a for measurements at station Hsinchu. The dimensionless water depth  $kh$  is also a function of  $x$ , see the broken line in Fig. 1a. Thus, equation (1) with variable coefficients is an appropriate basic model.

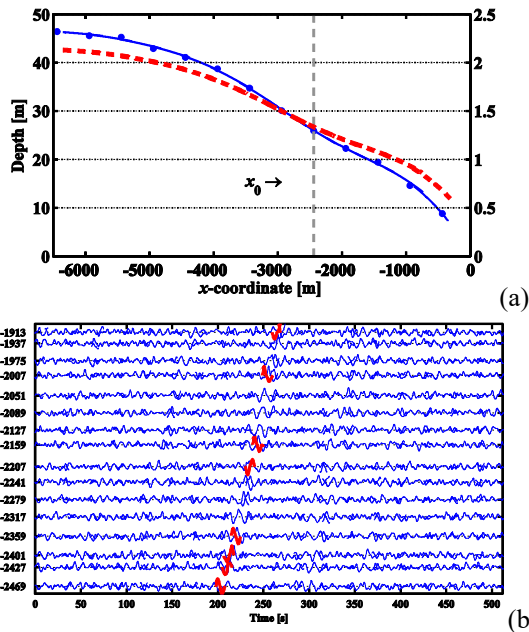


Fig. 1. The uneven bathymetry in the vicinity of the measurement by the Hsinchu buoy (a). The circles and the connecting line show the depth. The local dimensionless water depth  $kh$  is shown with broken line and corresponding right-side axis. The simulated rogue wave evolution in the vicinity of the buoy (b). Numbers at the left side give values of  $x$  in meters. The thick red curves show rogue waves with  $H/H_s > 2$ .

An example of the rogue wave reconstruction is shown in Fig. 1b. The time series are plotted for different locations. The rogue wave emerges a little bit prior the buoy location ( $x_0 = -2440$  m) and propagates for about 550 m during about 60 seconds, from time to time exceeding the conventional threshold of a rogue wave,  $2H_s$ .

Three more reconstructions of rogue waves from Taiwanese coasts may be found in Sergeeva et al (2014). A dozen more reconstructions were performed for time series from the North Sea at constant depth conditions (Slunyaev et al, 2005, 2014; Slunyaev, 2006). A more

accurate model, the modified NLSE (Dysthe equations), was used for that simulations. In many cases the anomalously high waves live relatively long, up to about 1-1.5 minutes.

### INDIRECT VALIDATION OF THE RECONSTRUCTION PROCEDURE AND POSSIBLE FORECASTING

In the reconstruction shown in Fig. 1 weakly nonlinear weakly modulated theory was employed, which is marginally applicable in situation of realistic sea storms. In this section we present a justification of the approach in the condition of infinitely deep water. The strongly nonlinear simulations of irregular sea waves with JONSWAP spectrum by means of the HOSM solver are used as the reference (the HOSM simulations are described in Sergeeva & Slunyaev, 2013). At some moment of the reference simulation the surface displacement  $\eta_{ref}(x, t^*)$  is taken and considered as it would be an instrumental record (the fluid velocity data is not used). The surface velocity potential is reconstructed at first, and the obtained initial condition is then simulated within different frameworks: the linear theory, the NLSE with full linear dispersion, and the Dysthe model with full linear dispersion.

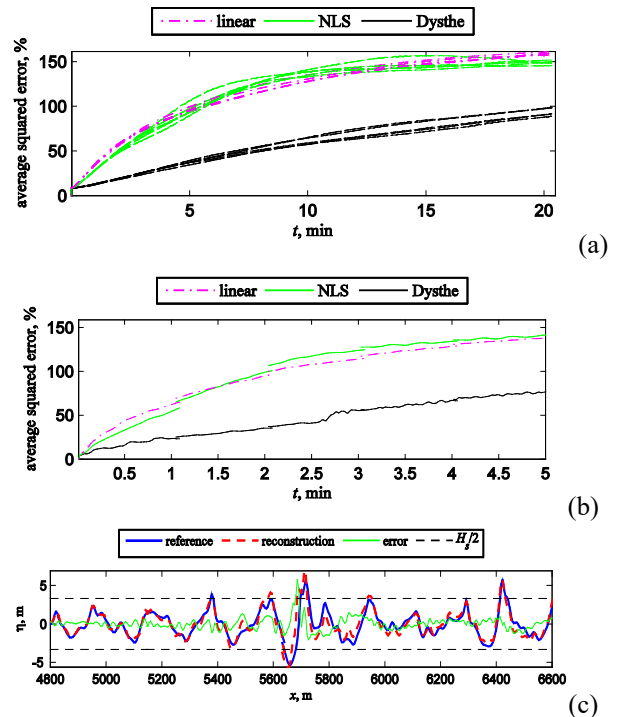


Fig. 2 Average difference (rms) in percents between the reference and the reconstruction for cases  $H_s = 3.5$  m ( $k_p H_s / 2 = 0.07$ ) (a) and  $H_s = 6.6$  m ( $k_p H_s / 2 = 0.13$ ) (b). An example of the most pronounced disagreement between surfaces for case  $H_s = 6.6$  m at  $t = 2$  min (c).

The reconstruction result (i.e. the simulated surface displacement  $\eta(x, t > t^*)$ ) is compared with the reference strongly nonlinear simulation  $\eta_{ref}(x, t > t^*)$ . The relative average squared errors for two sea conditions are shown in Fig. 2a,b. The first case is characterized by relatively smooth waves without breaking ( $H_s = 3.5$  m,  $T_p = 10$  s,  $\gamma = 3$ , five examples are shown in Fig. 2a), while in the second ( $H_s = 6.6$  m,  $T_p = 10.5$  s,  $\gamma = 3.3$ , Fig. 2b) waves occasionally break. The reconstruction rapidly gains a certain error due to the imperfect reconstruction of the

velocity field; later on the error grows much slower. One may conclude from Fig. 2a,b that the NLS framework practically has no advantage in comparison with the linear theory; in both the cases the reconstruction quickly depart from the reference. In the case of simulation of the Dysthe model the error is essentially smaller. In the steeper sea state (Fig. 2b) the error grows faster (note different scales in Figs. 2a, b). In Fig. 2c the wave interval is shown, which exhibits the maximal deviation between the reference and reconstruction. It corresponds to instant  $t = 2$  min of the steeper sea state simulation (Fig. 2b), when the average error is of order of 30%. One may see that the maximum excursion of the reconstructed wave corresponds to slightly different locations of waves, what in many cases may be practically insignificant. Thus, we may conclude that the time of reliable wave dynamics reconstruction from a given sea surface snapshot can be of order of a few minutes. Under another viewpoint, this estimate gives an idea about the feasible horizon of a deterministic forecasting of dangerous waves, when the simulation is used to foresee the wave evolution.

### NUMERICAL SIMULATIONS OF IRREGULAR NONLINEAR WAVES IN FINITE-DEPTH BASINS

The fast realistic numerical simulations of nonlinear surface waves help to obtain statistical information on sea waves which can be hardly obtained otherwise. In particular, the direct numerical simulations may be used to obtain the wave statistics for given sea states. We report here some results of simulations of quasi-stationary sea states. The initial conditions for the simulations are characterized by the JONSWAP spectrum; after a transient stage waves attain quasi-stationary state, and then the statistical data is collected (Sergeeva & Slunyaev, 2013; Slunyaev et al, 2016). The approach allows a twofold consideration: the traditional, based on time-series of the surface elevation; and the consideration of a spatial domain (snapshots), which is often preferable when waves are simulated in time. We show below that the wave statistics if time and space domains may look noticeably different.

The wave height exceedence probabilities for two different water depths  $k_p h \approx 2$  (Fig. 3a,b) and  $k_p h \approx 1.2$  (Fig. 3c,d) (where  $k_p$  denotes the peak wavenumber) and two characteristic wave steepnesses are presented in Fig. 3. The data in Figs. 3a-d corresponds to runs A<sub>2</sub>, E<sub>2</sub>, A<sub>1.2</sub> and E<sub>1.2</sub> from Slunyaev et al (2016). The blue and red lines correspond to down-crossing and up-crossing analysis respectively; the statistics in time domain is given by plane curves, while curves with dots denote the space domain consideration. The Rayleigh law is shown for reference by the green thick line, and the Glukhovskiy distribution (in original formulation) is given by magenta curves for time series and space series (solid and broken lines correspondingly).

One may see from Fig. 3 that the probability distributions for time series and space series exhibit rather different behaviour in the interval of large wave heights when water is deep (Fig. 3a, b); the difference is less evident in the shallower case  $k_p h \approx 1.2$  (Fig. 3c,d). The horizontal axes in Fig. 3 are scaled by the standard deviation of the surface elevation, which is the same for the consideration in time or space. The significant wave height, however, is dependent on the approach; it is somewhat larger for time series, since the frequency spectrum is narrower than the wavenumber spectrum, and thus the wave heights in time series diverse less than in space series. The mean wave heights also depend on the domain of analysis, what leads to different Glukhovskiy distributions (see solid and broken magenta curves in Fig. 3). The difference between Glukhovskiy distributions becomes smaller over shallower water (cf. Fig. 3a, c); it is interesting to note that

for steeper waves this difference diminishes to even a larger degree (see magenta curves in Fig. 3a,b, and also Fig. 3c,d).

The effect of nonlinearity on the wave height probability is evident from Fig. 3. In epy steeper sea state over deep water high waves are more frequent. The probability curves lie well below the Rayleigh law in Fig. 3c (intermediate depth, moderate wave steepness), they exceed the Rayleigh prediction when waves are rougher (Fig. 3b,d).

It is interesting to note that the up-crossing and down-crossing analyses exhibit significant difference in the steeper wave situations regardless the domain of consideration (time or space series), the probability distribution curves split in two in the large height interval, see Fig. 3b,d. This difference corresponds to a larger number of high crests with rear slopes deeper than their front slopes. This asymmetry of high waves in irregular seas was probably first mentioned in our work Sergeeva & Slunyaev (2013); it was also observed in 3D numerical simulations by Xiao et al (2013) and in in-situ data Pinho et al (2004).

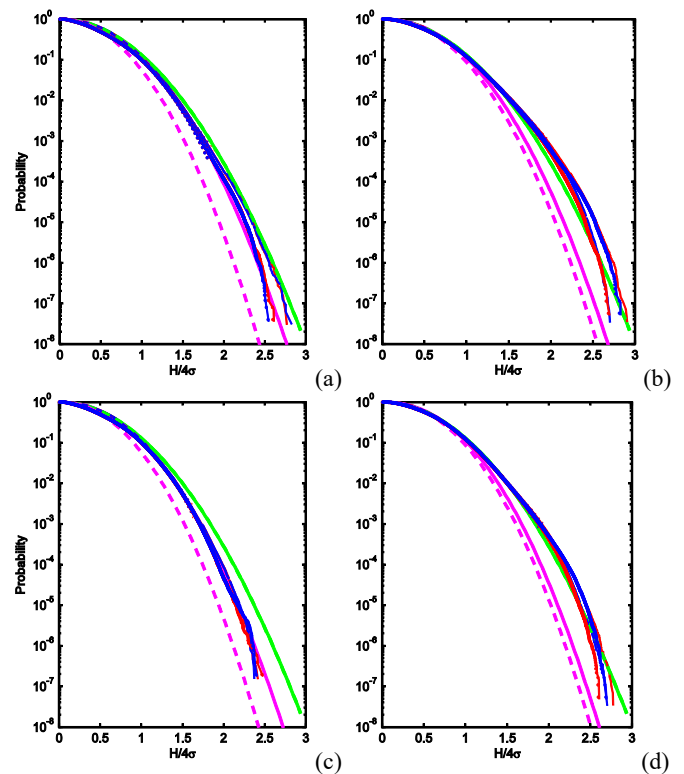


Fig. 3 Wave height exceedence probability distributions for two depths:  $k_p h \approx 2$  (a, b) and  $k_p h \approx 1.2$  (c, d) and two characteristic wave steepnesses:  $k_p H_s/2 = 0.07$  (a, c) and  $k_p H_s/2 = 0.13$  (b, d). See description in the text.

The maximum wave amplification  $H/4\sigma$  in the reported simulations is about 3. The probability distributions drop down at the maximum wave heights in Fig. 3 may be caused by the small number of events; in addition, the curves in Fig. 3b,d (steeper waves) may be affected by the employed regularization of eventual wave breaking.

Another promising application of the direct numerical simulations is related to obtaining the information on wave kinematics and pressures beneath the surface, which are extremely difficult to be measured in

laboratory facilities. The Monte-Carlo type simulations allow obtaining statistical data. The Eulerian surface velocities are given by formulas

$$V_x = \left. \frac{\partial \varphi}{\partial x} \right|_{z=\eta} = \frac{\varphi_x^s - \eta_x \eta_t}{1 + \eta_x^2}, \quad V_z = \left. \frac{\partial \varphi}{\partial z} \right|_{z=\eta} = \frac{\eta_t + \eta_x \varphi_x^s}{1 + \eta_x^2}. \quad (3)$$

These quantities were calculated for irregular waves over infinitely deep water in Sergeeva & Slunyaev (2013). It was concluded that the overlap between very high waves and waves with extreme kinematics is only partial. It was also noticed that the 3-order Stokes theory gives reasonable estimations for the maximum values of the surface velocities in relatively rough sea states.

The work by Sergeeva & Slunyaev (2013) was extended in Slunyaev et al (2016) to cases of finite depth basins, when waves start to ‘feel’ the bottom. The wave kinematics in the coastal area is probably of even greater importance than in the limit of infinite depth, thus we have considered how the fields of surface velocities depend on the depth.

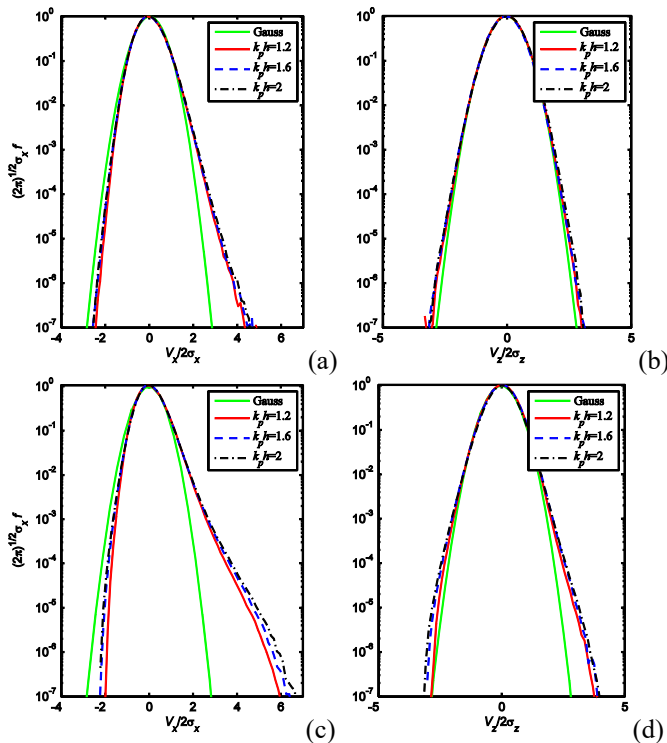


Fig. 4 Horizontal ( $V_x$ ) and vertical ( $V_z$ ) surface velocity probability densities for two characteristic wave steepnesses:  $k_p H_s/2 = 0.07$  (a, b) and  $k_p H_s/2 = 0.13$  (c, d), and three depths (see the legend).

The probability densities are calculated for  $V_x$  and  $V_z$ ; they are shown in Fig. 4. Two characteristic wave intensities are considered (Fig. 4a,b for moderate steepness and Fig. 4c,d for steeper waves) at three depths,  $k_p h \approx 2, 1.6$ , and  $1.2$  (see the legend). The normal (Gaussian) distribution is given for the reference as well.

A striking feature of Fig. 4 is that the curves for different depths collapse in one, and do not show any certain dependence on the depth (of course, the water is still not really shallow,  $k_p h \geq 1.2$ ). The probability density for the horizontal velocity is strongly asymmetric;

its tails depart essentially from the Gaussian curve. In the rougher case the right-hand tail of  $V_x$  has complicated dependence (Fig. 4c). At the same time, the vertical velocities  $V_z$  almost comply with the normal distribution in the case of moderate wave steepness (Fig. 4b); it becomes skewed when waves are steeper (Fig. 4d).

The probabilistic description of nonlinear wave kinematics is poorly developed so far. The presented examples of stochastic numerical simulations prove the efficiency of this approach for considering the wave statistics with minimal restrictions.

## ACKNOWLEDGEMENTS

Different aspects of this study are supported by different projects. The work towards analysis of extreme waves in coastal Taiwanese waters is supported by bilateral RFBR project 16-55-52019. The development of tools for short-term deterministic forecasting is supported by RSF grant No 16-17-00041. Stochastic simulations are conducted under support of RFBR projects 15-35-20563, 14-02-00983 and Volkswagen Foundation.

## REFERENCES

- Divinsky, B.V., Levin, B.V., Lopatukhin, L.I., Pelinovsky, E.N., Slunyaev, A.V. (2004) A freak wave in the Black sea: observations and simulation. *Dokl. Earth. Sci.* 395A, 438–443.
- Doong, D.J., Chen, S.H., Kao, C.C., Lee, B.C. (2007) Data quality check procedures of an Operational Coastal Ocean Monitoring Network. *Ocean Eng.* 34, 234-246.
- Dysthe, K., Krogstad, H.E., Müller, P. (2008) Oceanic rogue waves. *Annu. Rev. Fluid Mech.* 40, 287–310.
- Kharif, C., Pelinovsky, E. (2003) Physical mechanisms of the rogue wave phenomenon. *Eur. J. Mech./B – Fluid.* 22, 603–634.
- Kharif, C., Pelinovsky, E., Slunyaev, A. (2009) *Rogue Waves in the Ocean*. Springer-Verlag, Berlin Heidelberg.
- Pinho, U.F., Liu, P.C., Ribeiro, C.E.P. (2004) Freak waves at Campos Basin, Brazil. *Geofizika*, 21, 53-67.
- Sergeeva, A., Slunyaev, A. (2013) Rogue waves, rogue events and extreme wave kinematics in spatio-temporal fields of simulated sea states. *Nat. Hazards Earth Syst. Sci.* 13, 1759-1771.
- Sergeeva, A., Slunyaev, A., Pelinovsky, E., Talipova, T., Doong, D.-J. (2014) Numerical modeling of rogue waves in coastal waters. *Nat. Hazards Earth Syst. Sci.* 14, 861–870.
- Slunyaev, A. (2006) Nonlinear analysis and simulations of measured freak wave time series. *Eur. J. Mech./B – Fluid* 25, 621-635.
- Slunyaev, A., Didenkulova, I., Pelinovsky, E. (2011) Rogue Waters. *Contemp. Phys.* 52, 571-590.
- Slunyaev, A., Pelinovsky, E., Guedes Soares, C. (2005) Modeling freak waves from the North Sea. *Appl. Ocean Res.* 27, 12-22.
- Slunyaev, A., Pelinovsky, E., Guedes Soares, C. (2014) Reconstruction of extreme events through numerical simulations. *JOMAE* 136, 011302.
- Slunyaev, A., Sergeeva, A., Didenkulova, I. (2016, In Press) Rogue wave events in spatiotemporal numerical simulations of unidirectional waves in basins of different depth. *Nat. Hazards*. DOI: 10.1007/s11069-016-2430-x.
- Trulsen, K. (2001) Simulating the spatial evolution of a measured time series of a freak wave. In: Olagnon, M, Athanassoulis, G.A., (Ed.) Proc. ‘Rogue Waves 2000’, Brest, France, 265–274.
- Xiao, W., Liu, Y., Wu, G., Yue, D.K.P. (2013) Rogue wave occurrence and dynamics by direct simulations of nonlinear wave-field evolution. *J. Fluid Mech.* 720, 357-392.